Skeletal Radiology (2021) 50:1963–1980
https://doi.org/10.1007/s00256-021-03769-w

REVIEW ARTICLE

Magnetic resonance imaging of trunk and extremity myxoid liposarcoma: diagnosis, staging, and response to treatment

Asif Saifuddin[1] · Vanghelita Andrei[2] · Ramanan Rajakulasingam[1] · Ines Oliveira[3] · Beatrice Seddon[4]

Received: 22 February 2021 / Revised: 22 March 2021 / Accepted: 22 March 2021 / Published online: 1 April 2021

Abstract

Myxoid liposarcoma (MLS) accounts for approximately 30% of all liposarcomas. The majority are intermediate-grade tumours, but the presence of >5% round cell component renders it a high-grade sarcoma with subsequent poorer outcome. MLS most commonly arises in the lower extremities, has a predilection for extra-pulmonary sites of metastatic disease, and is recognized to be radiosensitive. The purpose of the current article is to review the role of MRI in the management of MLS, including the characteristic features of the primary tumour, features which help to identify a round cell component and thus determine prognosis, the role of whole-body MRI for evaluation of extra-pulmonary metastatic disease, and the utility of MRI for assessing treatment response. The MRI differential diagnosis of MLS is also considered.

Keywords Myxoid liposarcoma · MRI appearances · Staging · Treatment response

Introduction

Soft tissue tumours are sub-classified by the 2020 WHO Classification of Soft Tissue and Bone Tumours into benign, intermediate (locally aggressive), and malignant. Malignant tumours of adipocytic origin include well-differentiated liposarcoma (WD-LS) (NOS), myxoid liposarcoma (MLS including round cell sub-type), dedifferentiated liposarcoma (DD-LS), pleomorphic liposarcoma (PM-LS), and myxoid pleomorphic liposarcoma (M-PM-LS) [1, 2].

MLS is differentiated from other liposarcomas based on a variety of clinical and imaging features, including a relatively lower age at presentation, a predilection for the lower limbs, an unusual pattern of metastatic spread, and often quite specific MRI appearances. The purpose of the current article is to review the role of MRI in initial diagnosis, whole-body staging, response to neoadjuvant therapy and assessment of local and distant relapse based on a review of the current literature, with extensive illustrations from our own institutional experience.

Clinical aspects of myxoid liposarcoma

MLS is the second commonest sub-type of liposarcoma. In a study of 12,370 soft tissue sarcomas (STS) presenting to a single institution over a 10-year period, 1755 (14%) cases were liposarcomas of which 444 (25.3%) were MLS (including the round cell sub-type), all but 45 (10.1%) located in the trunk or extremities [3]. Similarly, in a study of 2170 patients extracted from the Surveillance, Epidemiology, and End Results (SEER) database with primary extremity liposarcoma diagnosed from 2004 to 2015, 711 (32.8%) were MLS [4].

✉ Ramanan Rajakulasingam
Ramanan.rajakulasingam1@nhs.net

Asif Saifuddin
Asif.saifuddin@nhs.net

Vanghelita Andrei
Vanghelita.andrei@nhs.net

Ines Oliveira
Ines.oliveira1@nhs.net

Beatrice Seddon
Beatrice.seddon@nhs.net

[1] Department of Radiology, Royal National Orthopaedic Hospital, Brockley Hill, Stanmore HA7 4LP, UK

[2] Department of Histopathology, Royal National Orthopaedic Hospital, Brockley Hill, Stanmore HA7 4LP, UK

[3] Department of Radiology, Northwick Park Hospital, Watford Road, Harrow HA1 3UJ, UK

[4] Department of Clinical Oncology, University College London Hospital, 250 Euston Road, London NW1 2PG, UK

Lansu et al. [5] reported on 901 patients with MLS diagnosed in the Netherlands from 1989 to 2016, of which 512 (57%) were males and 389 (43%) females, the median age at diagnosis being 49 years (interquartile range: 38–62 years). Once again, 815 (91%) cases involved the trunk or extremities, of which 53 (6.5%) involved the upper limb, 577 (70.8%) the lower limb (mainly the thigh), and 185 (22.7%) the trunk [5]. MLS tends to have an intramuscular or intermuscular location as opposed to the subcutaneous soft tissues [6].

MLS is the commonest sub-type of liposarcoma occurring in young patients. Alaggio et al. [6] reported on 82 liposarcomas in patients under 22 years of age, 56 (68.3%) of which were typical MLS, 2 of which had a round cell (RC) component and 6 further cases reported as 'spindle cell MLS'. In the study by Lansu et al. [5], 352 (39%) patients were aged <40 years, while only 68 (7%) were > 70 years old.

MLS typically presents as a slow-growing, painless, deep tumour in the lower extremity. Due to the lack of symptoms, it tends to be relatively large at diagnosis with a median tumour size of 12 cm [7]. Metastatic disease at diagnosis is reported in 6% of patients [5].

By comparison, retroperitoneal MLS is rare with only a single case identified in a study of 131 primary retroperitoneal sarcomas [8]. However, a further study of 19 retroperitoneal liposarcomas identified 9 MLS, 2 of which had a round cell component [9]. Due to its rarity, it is difficult to comment on prognosis. However, it should also be noted that some authors do not believe that primary retroperitoneal MLS exists and that all such cases are metastatic [10].

Pathology of myxoid liposarcoma

Histologically, MLS is a multinodular tumour of low-to-intermediate cellularity with a prominent myxoid stroma which is rich in hyaluronic acid and has a characteristic plexiform vasculature (the so-called 'chicken-wire' vasculature). The neoplastic cells are monotonous, small, and round to ovoid. Lipoblasts are easily identified, but their identification is not required for diagnosis (Fig. 1). Occasional metaplastic cartilaginous and osseous elements can be seen, and molecular studies have shown that these components have the same molecular alterations as the liposarcomatous area [2, 11, 12]. High-grade MLS is defined as >5% of the tumour having a round cell (RC) component [2]. This consists of hypercellular areas with overlapping nuclei showing cells with round morphology and a high nuclear/cytoplasmic ratio (Fig. 2) [13]. The myxoid matrix is reduced and the vasculature is covered in these areas. It is important to distinguish the high-grade component from the increased cellularity which is usually present at the periphery of the tumour nodules, especially on needle biopsy. The presence of a RC component is associated with a greater risk of metastatic disease and an overall adverse outcome [14, 15].

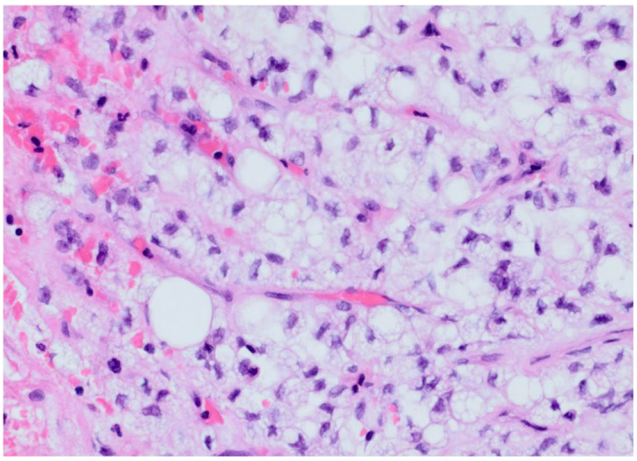

Fig. 1 H&E (200x magnification) showing a moderately cellular tumour composed of relatively monomorphic ovoid cells embedded in a myxoid stroma, with intervening branching capillary vessels. The tumour has a lobular architecture, and increased cellularity is seen at the periphery of the lobules, but these do not amount to a high-grade component

Immunohistochemistry is of no value in diagnosing this neoplasm. The pathogenesis of MLS and its RC sub-type is characterized by a translocation between chromosomes 12 and 16, resulting in the fusion of the *DDIT3* gene on chromosome 12 with the *FUS* gene on chromosome 16. In a small number of cases, the *EWSR1* gene on chromosome 22 can be involved, resulting in *EWSR1-DDIT3* fusion [2]. Consequently, FISH assay with *DDIT3* break-apart probe is a sensitive and specific marker for MLS [16].

MLS is a radiosensitive tumour, the pathological response including hyalinization, fibrosis, decline in cellularity, and adipocytic maturation in the majority of cases (Fig. 3) [17–19].

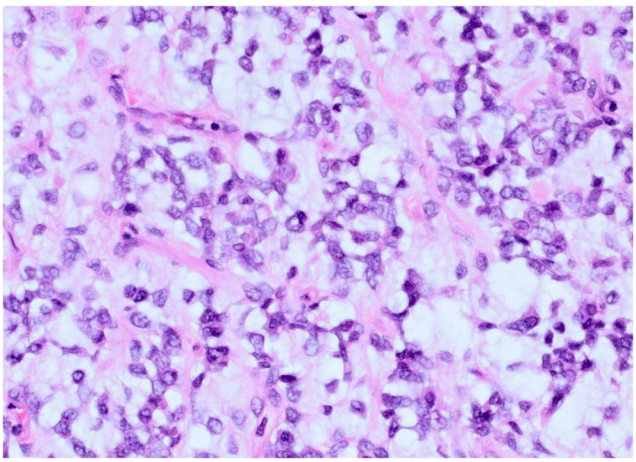

Fig. 2 H&E (200x magnification) showing a tumour composed predominantly of undifferentiated round cells with large nuclei and prominent nucleoli

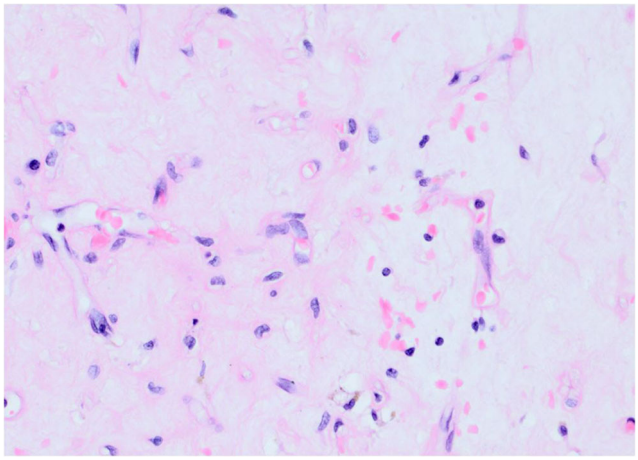

Fig. 3 H&E (200x magnification) showing a myxoid liposarcoma with diffuse post-radiotherapy changes, including decrease in cellularity and adipocytic maturation

MRI features of myxoid liposarcoma: the primary tumour

Table 1 summarizes the findings from several studies that have compared the MRI appearances of various sub-types of liposarcoma [20–22]. Barile et al. [20], El Ouni et al. [21], and Wortmann et al. [22] showed WD-LS to be a predominantly T1W high-signal intensity (SI) mass with low T1W SI septa. However, MLS was mildly heterogeneous with predominantly high SI on T2W images and isointense T1W SI compared to skeletal muscle, with lacy/linear septa of fatty tissue (Figs. 4, 5) [20–22]. El Ouni et al. [21] also demonstrated that a small amount of fatty tissue producing a 'marbled textural pattern' on T1W images was particularly prevalent in MLS, as well as distinct non-lipomatous elements in high-grade liposarcomas (RC-MLS and in 2 of 3 PM-LS). Overall, these studies would suggest that MLS commonly has a characteristic MRI appearance (Fig. 6), allowing a prospective MRI diagnosis in 78–95% of cases [23]. An additional MRI feature which may suggest the presence of high-water content in a superficial soft tissue mass is chemical shift artefact at the lesion margin. This has been described with MLS (Fig. 7) but is non-specific, being seen in a wide variety of superficial non-neoplastic, benign neoplastic, and malignant neoplastic lesions [24].

Sundaram et al. [25] describe 7 cases of MLS, MRI showing the tumours to be encapsulated, non-infiltrating, and usually septated. Most lesions were typically low-intermediate SI on T1W images, with 5 lesions (71%) demonstrating lacy, amorphous, or linear foci of hyperintensity within a low SI mass considered to represent fat. Sung et al. [26] described a spectrum of MRI findings in MLS depending upon the relative amount of fat and myxoid tissue, the degree of cellularity and vascularity, and the presence or absence of necrosis. Most MLS contained lacy, linear, or amorphous foci of fat (Figs. 4,5,6). Some appeared cystic on non-enhanced MRI (Fig. 7), although they enhanced like other solid masses on post-contrast imaging. The enhancing areas within the tumour corresponded to increased cellularity and vascularity (Fig. 8), while the non-enhancing areas represented necrosis, reduced cellularity, and accumulated myxoid material. Gadolinium-enhanced MRI was highlighted for its importance in differentiating MLS from benign cystic tumours. In this respect, Lunn et al. [27] described the differentiating MRI features between MLS ($n = 16$) and intramuscular

Table 1 Literature summarizing MRI features differentiating well-differentiated liposarcoma/atypical lipomatous tumour from myxoid liposarcoma

Study (Ref.)	No. of cases	Description
MRI features of WD-LS/ALT		
Barile et al. [20]	7	Predominantly homogenous fatty SI mass in all cases with non-lipomatous T1W isointense and T2W hyperintense SI septa ± nodularity
El Ouni et al. [21]	3	As above
Wortman et al. [22]	10	T1W hyperintense signal in 8; isointense in 2 T2W hyperintensity in all
MRI Features of MLS		
Barile et al. [20]	9	Mildly heterogeneous, predominantly fluid SI mass. Fatty SI septa/nodular foci appearing as lacy, linear, or amorphous foci of fat in 6 cases
El Ouni et al. [21]	12	Mildly heterogeneous, predominantly non-fatty SI mass. T1W 'marble textured pattern' in 9 cases
Wortman et al. [22]	28	Predominantly T1W isointense to skeletal muscle in all cases and T2W hyperintense myxoid SI
Sundaram et al. [25]	7	Fatty SI septa/nodular foci which can appear as lacy, linear, or amorphous foci

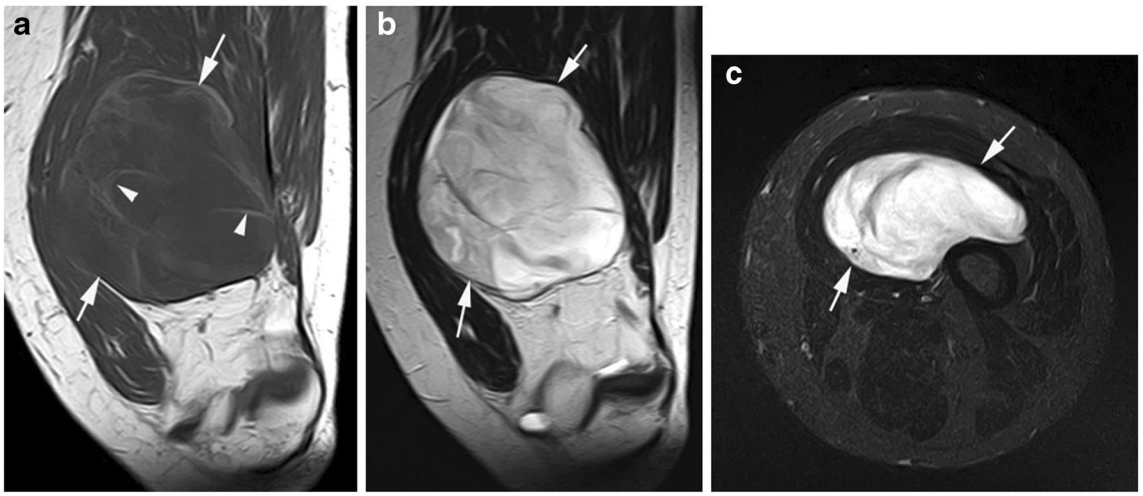

Fig. 4 A 47-year-old male presenting with a mass in the anteromedial aspect of the distal left thigh. **a** Coronal T1W TSE, **b** coronal T2W FSE, and **c** axial STIR MR images show a well-defined, lobular mass (arrows) which is isointense to muscle on T1W and hyperintense on T2 and STIR. The lesion contains thin mildly hyperintense septal fat on T1W (arrowheads-a) and has a thin hypointense capsule with hypointense internal septa on T2W and STIR. Histology confirmed myxoid liposarcoma with no round cell component

myxomas ($n = 8$). MLS occurred in younger patients (mean age 42.8 ± 16.3 years compared to 65.6 ± 10.4 years: $p = 0.0015$) and were larger (16.4 ± 8.2 vs. 5.6 ± 2.5 cm; $p = 0.0015$) and more commonly T1 hyperintense ($p = 0.03$), with nodular enhancement ($p = 0.006$) and macroscopic fat ($p = <0.001$) compared to myxomas. Of interest, this study also found no differentiating features between MLS and myxomas on ^{18}F-FDG PET/CT.

MRI features which may have prognostic value in MLS were the subject of several studies [28–30]. Tateishi et al. [28] reviewed 36 patients with histologically confirmed MLS, aiming to determine which MRI features best indicated tumours with adverse clinical behaviour. MRI findings that favoured a diagnosis of intermediate-grade or high-grade MLS were larger tumour size (>10 cm) (Figs. 9, 10), deep location, tumours with irregular contour, the absence of lobulation, thin septa and a tumour capsule, the presence of thick septa, a high-intensity signal pattern, pronounced enhancement, and globular or nodular enhancement. Univariate analysis showed that thin septa ($p < 0.05$), presence of a tumour capsule ($p < 0.01$), and pronounced enhancement ($p < 0.01$) were all significantly associated with overall survival, while multivariate analysis showed that pronounced enhancement was the most significant adverse prognostic factor. Kuyumcu et al. [29] undertook a study to determine the fat content of MLS on MRI and to see if there was any association between lipid content and survival. A lipid-rich MLS was arbitrarily defined as one which had >20% fat content on MRI. Of the 43 case studies, 8 demonstrated ≥10% fat on MRI, and 4 tumours demonstrated ≥20% fat, the highest fat content measured at 38%. There was no significant survival difference between patients with lipid-rich as opposed to lipid-poor MLS. Crombé et al. [30] investigated the additional value of radiomics to standard MRI assessment in MLS with the aim of improving patient prognosis. A total of 35 patients with pretreatment contrast-enhanced MRI were reviewed, and they concluded that adding selected radiomics features that quantify tumour heterogeneity and shape at baseline to conventional radiological analysis improved the prediction of patient prognosis in MLS.

Table 2 highlights the differing MRI appearances of MLS and MLS with a RC component. The latter is seen in 9% of MLS, and patients with RC tumours are significantly older as compared to patients with intermediate-grade MLS (median age 53 vs. 48 years, respectively; $p = 0.01$) [5]. The strongest adverse prognostic factor in MLS is the presence of a RC component comprising >5% of tumour bulk. However, identification of RC-MLS is underestimated on needle biopsy and following neoadjuvant treatment [30]. Therefore, MRI features predictive of a > 5% RC component may be of value, as while not affecting primary management, it does give an indication of expectations for the future in terms of the higher risk of developing metastatic disease. As such, studies have also been undertaken with the aim of differentiating low-grade from high-grade MLS, the latter defined as having >5% RC component [31, 32]. Löwenthal et al. [31] evaluated 30 MLS, 19 of which were diagnosed as low-grade and 11 high-grade. The mean tumour volume of low-grade MLS (710.1 ± 960.1 cm^3) was significantly smaller than high-grade MLS (2737.0 ± 3423.7 cm^3; $p = 0.04$). In addition to necrotic areas, 3 distinct tumour components were evident on MRI – fatty, myxoid, and contrast-enhancing non-fatty, non-myxoid areas (Fig. 10). The mean fraction of

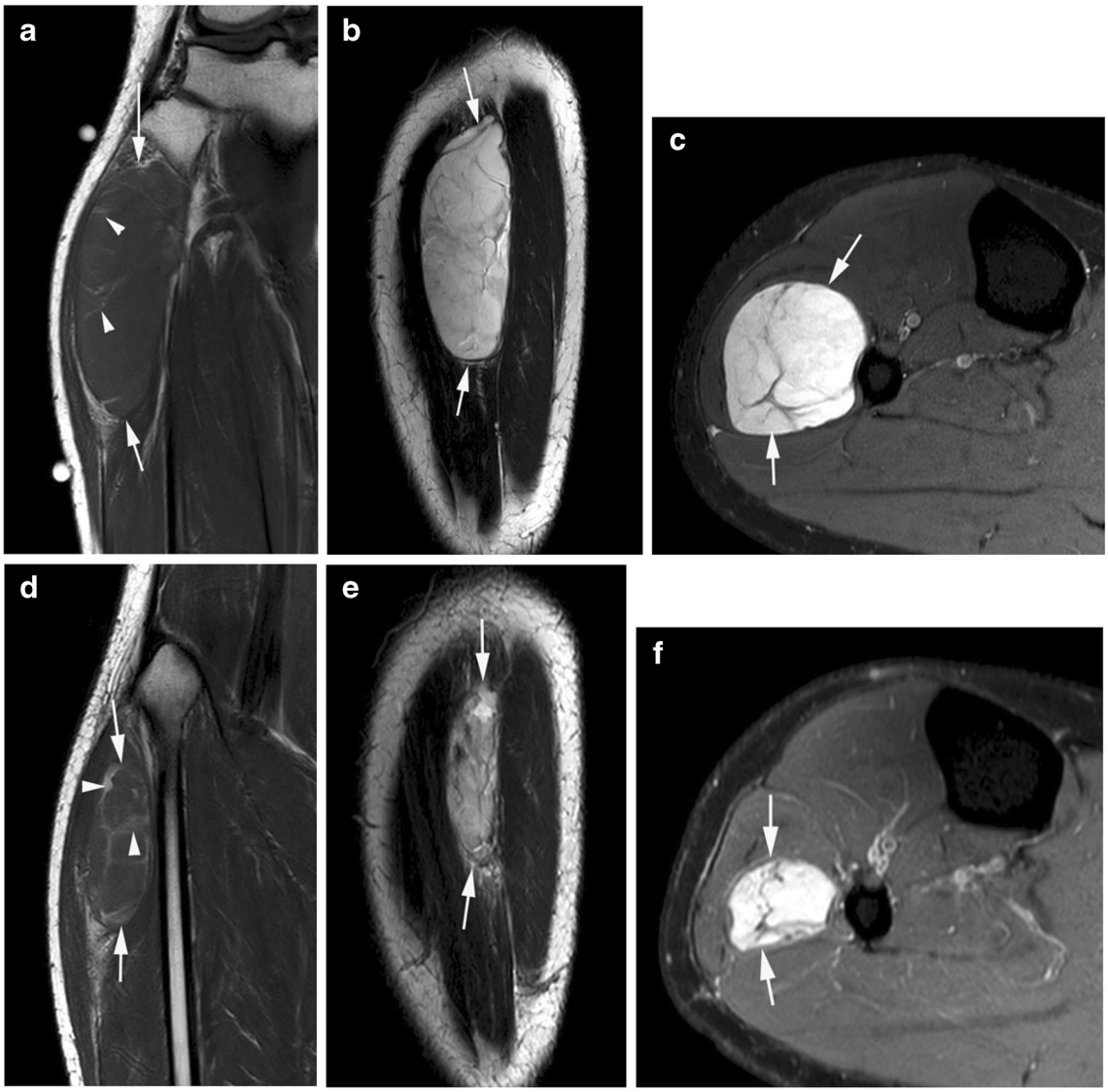

Fig. 5 A 43-year-old male presenting with a mass in the lateral aspect of the right proximal calf. **a** Coronal T1W TSE, **b** sagittal T2W FSE, and **c** axial SPAIR MR images show a well-defined, elongated mass (arrows) which is isointense to muscle on T1W and hyperintense on T2 and STIR. The lesion contains thin septal fat on T1W (arrowheads-a) and has a thin hypointense capsule with hypointense internal septa on T2W and SPAIR. **d** Coronal T1W TSE, **e** sagittal T2W FSE, and **f** axial SPAIR MR images obtained 3 months later following neoadjuvant radiotherapy which resulted in a 74% volume reduction of the mass (arrows) with maturation of the septal fat (arrowheads). Histology confirmed myxoid liposarcoma with no round cell component

fatty tumour in low-grade MLS was 10 ± 11% compared to 6 ± 4% for high-grade MLS ($p = 0.66$), while myxoid components accounted for 88 ± 16% in low-grade MLS compared to 45 ± 25% in high-grade MLS ($p < 0.0001$). The non-fatty, non-myxoid tumour component was significantly higher in high-grade MLS (50 ± 25%) as compared to low-grade MLS (2 ± 9%; $p < 0.0001$). A proportion of >5% of this tumour component was found to be an accurate predictor for high-grade MLS with a sensitivity of 100% and a specificity of 95%. A similar study was undertaken by Gimber et al. [32], who assessed 31 patients with MLS (23 low-grade, 8 high-grade). All high-grade lesions had lipid signal, a peri-tumoral capsule and peri-tumoral contrast enhancement, and more commonly exhibited heterogeneous SI **(**Figs. 9,10**)**. However, a mean size of ≥10 cm was the strongest independent indicator of high-grade MLS (odds ratio 14.6). Solid appearing non-fatty/non-myxoid tissue should be specifically targeted, possibly together with a more typical area of MLS at the time of needle biopsy to increase the chances of diagnosing a RC component.

The MRI features of retroperitoneal MLS are identical to extremity and trunk MLS, the tumour showing predominantly fluid SI characteristics on T1W and T2W sequences, while appearing more solid and heterogeneous in the presence of a round cell component [9, 33].

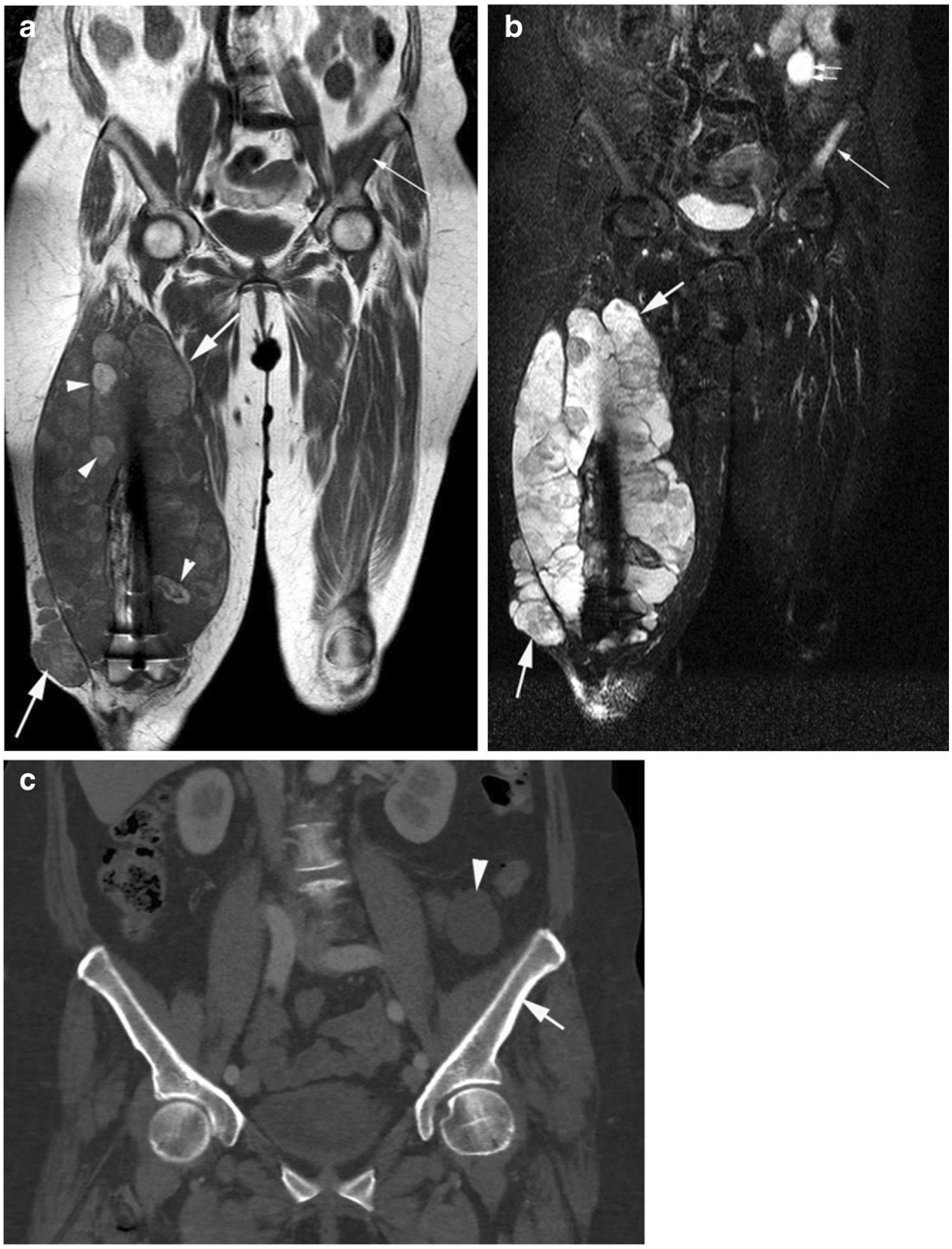

Fig. 6 A 70-year-old female presenting with a huge mass in the right thigh with previous history of femoral intramedullary nailing for a diaphyseal fracture. **a** Coronal T1W TSE and **b** coronal STIR MR images from a whole-body study show a large, poorly defined, lobular mass (arrows) which is predominantly isointense to muscle on T1W and heterogeneously hyperintense on STIR. The lesion contains multiple areas of nodular T1W hyperintensity (arrowheads-a) consistent with fat and also a left iliac metastasis (thin arrows) as well as a suspected left-sided intra-abdominal soft tissue metastasis (double arrow-b). **c** Coronal CT of the lower abdomen shows the fluid density intra-abdominal mass (arrowhead), but the left iliac blade lesion is not evident (arrow). Histology from needle biopsy confirmed myxoid liposarcoma with no round cell component

Patterns and detection of metastatic disease

Evidence of distant metastases at diagnosis of MLS is reported as being between 0.7 and 6% [6, 7, 11–14, 19]. However, this is likely to be an underestimate since it was not based on whole-body MRI, and it is recognized that metastases may be clinically silent in many cases.

Patterns of metastatic spread/late recurrence in MLS have been reported in several studies [34–39]. Pearlstone et al. [34] reviewed 122 patients with intermediate-grade or high-grade extremity liposarcoma of all sub-types, 102 patients (84%) having MLS. Of these, 33 (27%) had distant recurrences of which 31 (93.9%) were to extra-pulmonary soft tissue sites and 2 were to the lung only. This differed significantly from 18 patients with PM-LS, 10 (55.6%) of whom had distant recurrences with only 3 at extra-pulmonary sites and 7 in the lung only. Estourgie et al. [35] identified metastatic disease in 22 of 128 (17.2%) patients with extremity liposarcoma of all histological sub-types (49 MLS) studied over a 20-year period with a mean follow-up of 45 months. Of these, extra-pulmonary metastases developed in 10 (45.5%), combined pulmonary and extra-pulmonary metastases in 6 (27.3%),

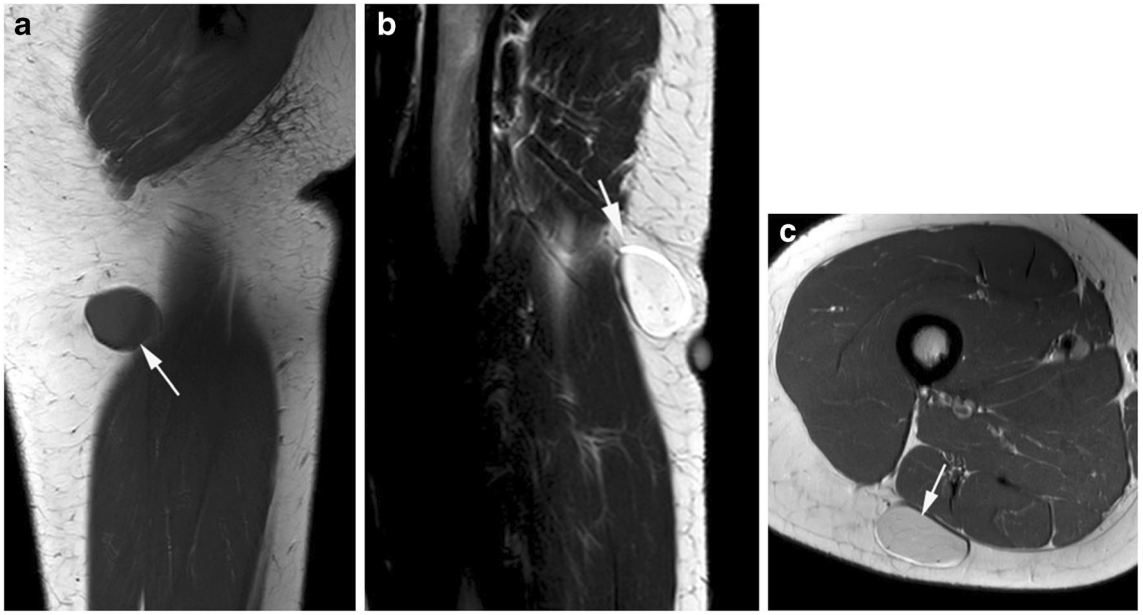

Fig. 7 A 26-year-old female presenting with a small mass in the posterior aspect of the right thigh. **a** Coronal T1W TSE, **b** sagittal T2W FSE, and **c** axial PDW FSE MR images show a small well-defined superficial mass (arrows) which has no distinguishing features. Note the presence of chemical shift artefact at the lesion margin. Histology confirmed myxoid liposarcoma with no round cell component

and isolated pulmonary metastases in 6 (27.3%). Of the 16 patients with extra-pulmonary metastases, 13 (81.3%) were MLS. Of the 49 patients with extremity MLS, metastases developed in 14 (29%), the commonest sites being the retroperitoneum ($n = 10$; 71%) (Fig. 11), intra-abdominal extrahepatic ($n = 7$; 50%) (Fig. 6), and spinal/paraspinal ($n = 6$; 43%) (Figs. 12,13). Only 3 patients were alive and disease-free, all of these being from the sub-group of 10 patients with only extra-pulmonary metastases (2 intra-abdominal and 1 retroperitoneal). Schwab et al. [36] investigated the incidence and outcome of bone metastases in 230 patients with MLS, of whom 40 (17%) developed skeletal metastases, comprising 56% of all metastatic lesions. Bone metastases were commonly identified early in the disease course, the commonest location being the spine. From the time of first metastasis, the median 5-year survival was 16%, 78% of patients having high-grade MLS. The median overall survival for the high-grade tumours was 55 months compared to 105 months for low-grade cases. Asano et al. [37] reviewed 58 cases of MLS, 11 patients (19%) having metastases during their clinical

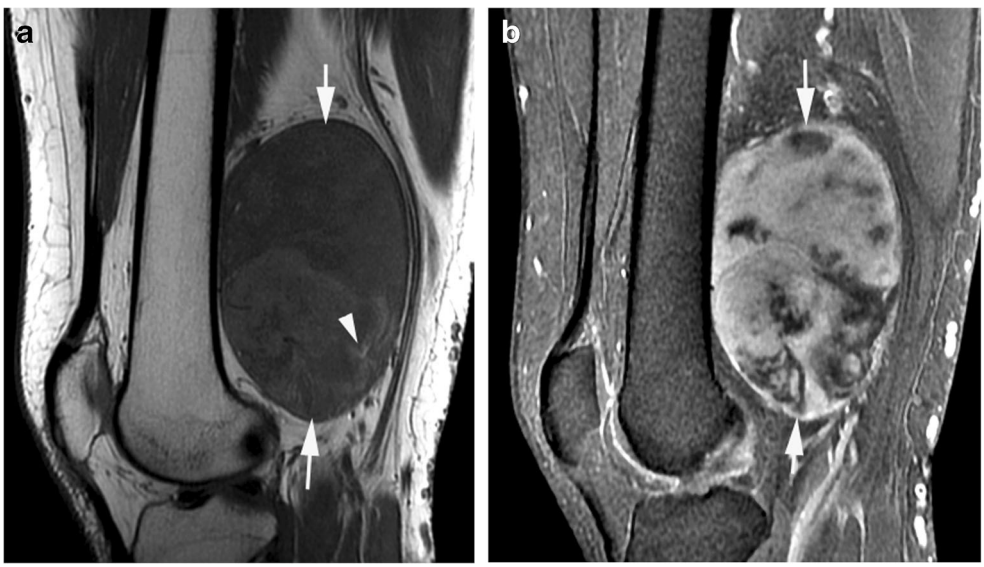

Fig. 8 A 37-year-old male presenting with a mass in the posterior aspect of the distal thigh. **a** Sagittal T1W TSE and **b** sagittal fat suppressed post-contrast T1W TSE MR images show a well-defined oval mass (arrows) in the popliteal fossa deep to the vessels. The lesion has heterogenous intermediate SI on T1W with a small area of fat (arrow). The lesion demonstrates heterogeneous enhancement following contrast. Histology confirmed myxoid liposarcoma with no round cell component

Fig. 9 A 55-year-old male presenting with a large mass in the right popliteal fossa. **a** Coronal T1W TSE, **b** sagittal T2W FSE, and **c** axial SPAIR MR images show a well-defined, lobular mass (arrows) which shows markedly heterogeneous SI on all pulse sequences. Histology confirmed myxoid liposarcoma with a round cell component

course. Of these, 8 (73%) had extra-pulmonary metastases, and 3 patients (27%) had pulmonary metastases. Patients were further subdivided into 3 groups: those without metastasis, those with extra-pulmonary metastasis, and those with pulmonary metastasis. When the metastatic patterns were stratified based on tumour size, there was statistical significance found ($p = 0.028$) with the 8 cases having extra-pulmonary metastases all being >10 cm. Similarly, histological grade had a significant impact on metastatic patterns ($p = 0.027$), the 3 cases with pulmonary metastases all being high-grade MLS. Therefore, large tumour size and low-grade histology were significantly associated with extra-pulmonary metastatic

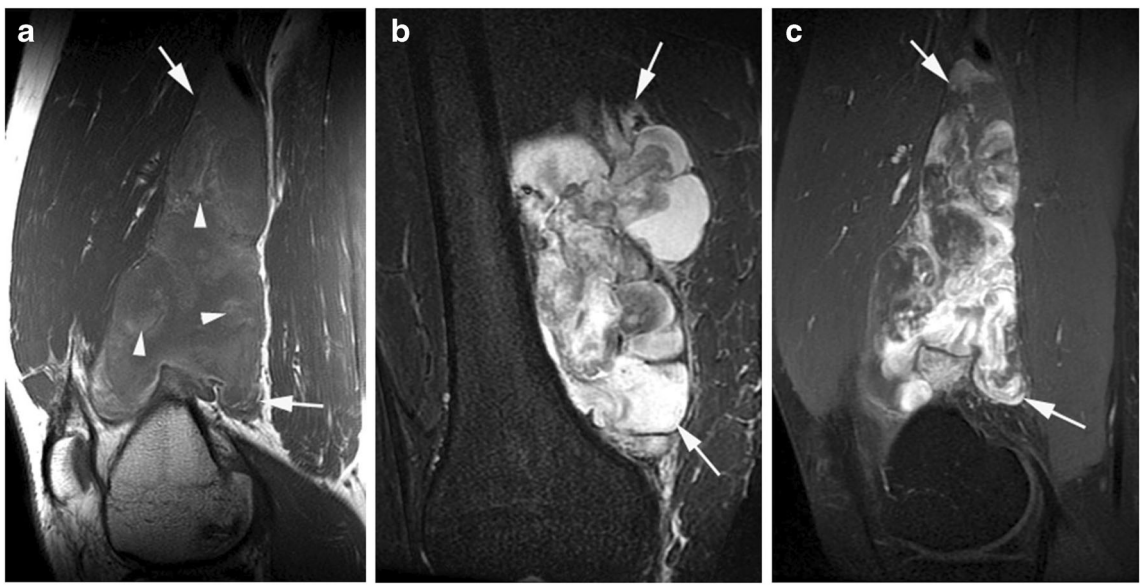

Fig. 10 A 24-year-old male presenting with a mass in the medial aspect of the right distal thigh. **a** Sagittal T1W TSE, **b** coronal STIR, and **c** sagittal fat suppressed post-contrast T1W TSE MR images show a poorly defined, lobular mass (arrows) located between the femur and the vastus medialis muscle. The lesion contains multiple areas on internal T1W hyperintensity (arrowheads-a) and extensive areas of non-fatty/non-myxoid tissue on STIR, showing heterogeneous enhancement following contrast. Histology confirmed myxoid liposarcoma with a round cell component

Table 2 Literature summarizing differing MRI appearances of myxoid liposarcoma and myxoid liposarcoma with a round cell component

Features of MLS	Features of MLS+round cell component
Younger patient age (median 48 years) [5]	Older patient age (median 53 years) [5]
No significant non-myxoid areas [20–22, 31]	Separate areas of necrosis, fatty, myxoid, and contrast enhancing non-fatty, non-myxoid areas [31]
No peri-tumoral enhancement [28]	Peri-tumoral capsule and contrast enhancement [28, 32]
Mean size <10 cm [28]	Mean size >10 cm [28, 32]

spread. Dürr et al. [38] reported on 43 patients with MLS (25 thigh, 9 calf, 5 popliteal region, 1 foot, 1 upper arm, and 2 trunk), only 3 (7%) have metastases at the time of initial surgery, and these were located in the retroperitoneum, lumbar spine, and pelvic lymph nodes. Smolle et al. [39] identified MLS as being the commonest soft tissue sarcoma to metastasize to the retroperitoneum or abdomen; this is seen in 12.1% of cases.

Specific sites of metastases in MLS have been identified in numerous cases reports, including the skeleton (Figs. 14,15) [40, 41], the skull base [42], the heart [43] and pericardium [44, 45], the breast [46], pancreas [47], thyroid gland [48], and peritoneum [49]. The median time from diagnosis of the primary tumour to a developing new metastatic disease is around 2–3 years [15, 50], although there are many reports of late metastatic events, for example, 16 years [45].

The imaging features of metastatic MLS have been the subject of several reports [51–53]. Sheah et al. [51] described the MRI, CT, and FDG-PET features of 23 histologically proven metastases in 12 patients with MLS, although by imaging criteria, there were 41 metastatic deposits. The mean time from diagnosis to first metastasis was 4.4 years. Two-thirds of patients had bone and soft tissue metastases (Fig. 15), 33% lung metastases, 33% liver metastases, 25% intra-abdominal, and 16% retroperitoneal metastases. CT demonstrated well-defined lobular masses with soft tissue attenuation in

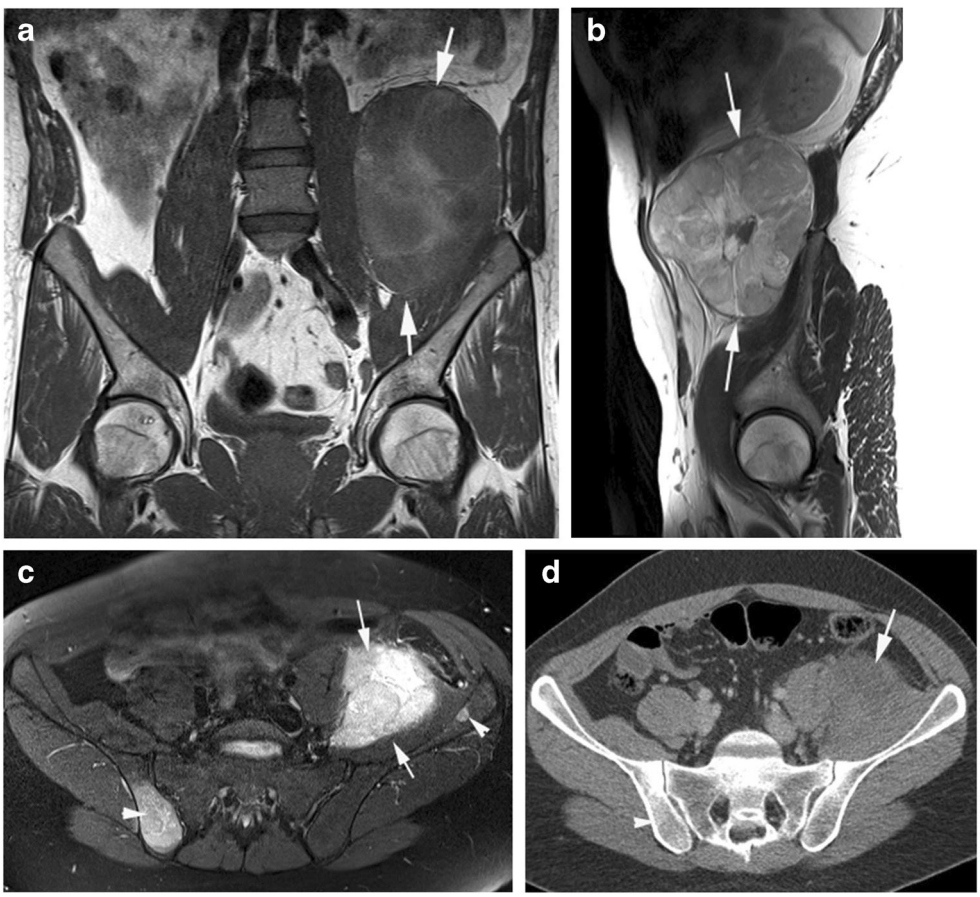

Fig. 11 A 30-year-old female presenting with a left abdominal mass and a previous history of myxoid liposarcoma of the calf 1 year earlier. **a** Coronal T1W TSE, **b** sagittal T2W FSE, and **c** axial SPAIR MR images show a large, lobular, haemorrhagic left retroperitoneal mass (arrows) and bone metastases (arrowheads) in the iliac blades. **d** Axial CT study shows the soft tissue mass (arrow) but the bone lesions (arrowhead) are not identified. Resection of the retroperitoneal mass confirmed metastatic myxoid liposarcoma

Fig. 12 A 72-year-old female presenting with a mass in the posterior aspect of the left lumbar region. **a** Sagittal T1W TSE, **b** sagittal STIR, and **c** axial T2W FSE MR images show a large poorly defined deep mass (arrows) which is eroding bone and extending into the spinal canal. A focal marrow lesion (arrowheads-a, b) is present in T10. **d** Sagittal and **e** axial CT images show no lesion at the T10 level (arrows). Histology confirmed myxoid liposarcoma with no round cell component

all cases (Fig. 11d), without a macroscopically evident fat component. In the cases of bone metastases, CT showed mixed lytic and sclerotic foci, with bone destruction in advanced cases. MRI demonstrated fluid SI (Figs. 14,15) with mild heterogeneous enhancement in soft tissue metastases, while bone metastases showed marked heterogeneous enhancement. FDG-PET showed no significant FDG uptake for all metastases. Noble et al. [52] described the features of bone metastases in 8 patients with MLS, this representing 4.3% of their study population. All were identified on MRI, while bone scintigraphy was negative in 2 of 4 cases (Fig. 16), CT was negative in 6 of 7 cases (Figs. 6c, 11d, 12d, e), and radiographs were negative in 4 patients. They concluded that when investigating patients with MLS for bone pain, negative

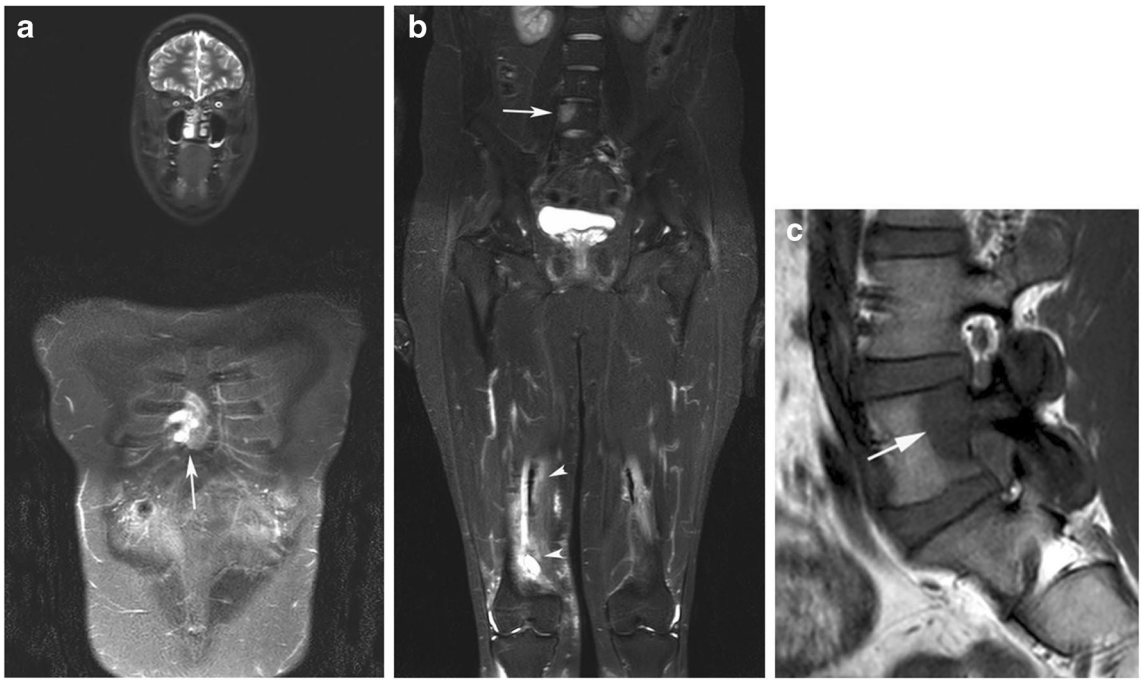

Fig. 13 A 26-year-old male presenting with a sternal mass having been treated for myxoid liposarcoma of the right thigh 1 year previously. **a**, **b** Coronal STIR MR images from a whole-body MRI study demonstrate lesions arising from the right lower sternum with soft tissue extension (arrow-a) and from the right side of the L5 vertebral body (arrow-b). Post-treatment changes are noted in the medial right thigh (arrowheads-b). (c) Sagittal T1W TSE MR image confirms marrow replacement (arrow) in the right posterior L5 vertebral body extending into the pedicle and L5-S1 foramen. Biopsy of the parasternal mass confirmed metastatic myxoid liposarcoma

radiographs and bone scans do not rule out bone metastases. Schwab et al. [53] reported specifically on their experience of spinal metastases in MLS, identified in 33 of 230 (14.3%) cases. Of these, 29 were symptomatic while in 4 cases, the spinal lesion was an incidental finding. A total of 17 patients had >1 spinal region involved, the commonest site of metastasis being the lumbar spine (Fig. 13) ($n = 23$), followed by the thoracic spine (Fig. 12) and sacrum (Fig. 16) ($n = 19$ and 8,

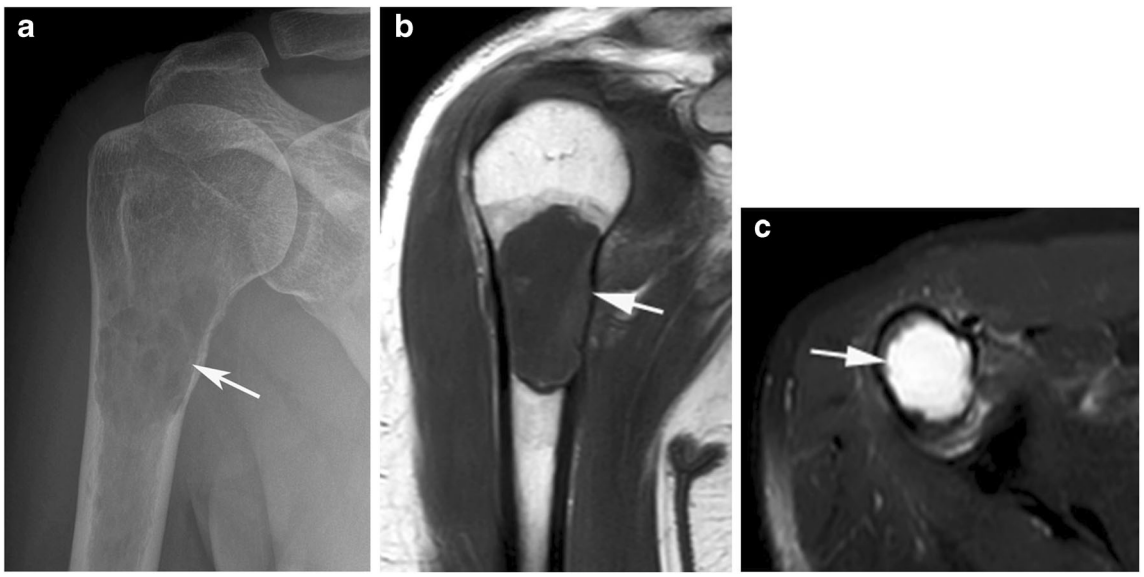

Fig. 14 A 31-year-old male presenting with right upper arm pain and a previous history of high-grade myxoid liposarcoma of the right thigh 2 years earlier. **a** AP radiograph of the right shoulder shows an aggressive lytic destructive lesion (arrow) in the proximal humeral metaphysis. **b** Coronal T1W TSE and **c** axial SPAIR MR images show a lobular fluid SI lesion (arrows) in the proximal humeral metaphysis consistent with a metastasis. Biopsy proven myxoid liposarcoma metastasis

Fig. 15 A 61-year-old male with a history of myxoid liposarcoma of the right lower leg 4 years earlier. **a** Coronal T1W TSE, **b** coronal STIR, and **c**, **d** axial SPAIR MR images show multifocal fluid SI bone (arrows) and soft tissue (arrowheads) lesions consistent with myxoid liposarcoma metastases

respectively) and least commonly the cervical spine ($n = 4$). The epidural extension was seen in 16 cases. Compared to MRI, spinal metastases were detected on bone scintigraphy in 16% of patients and by FDG-PET in 14% of patients. The relative insensitivity of CT and scintigraphy, including FDG-PET, compared to MRI, has been noted in several other

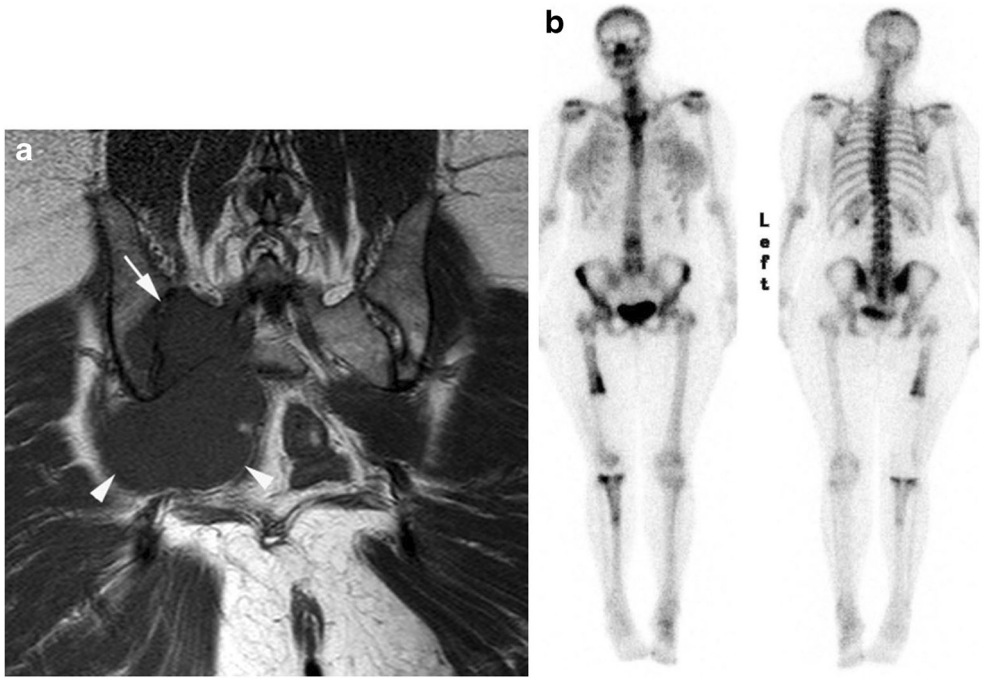

Fig. 16 A 50-year-old female presenting with right buttock pain and a previous history of myxoid liposarcoma of the right thigh 4 years earlier. **a** Coronal T1W TSE MR image shows marrow infiltration in the right sacral ala (arrow) with extra-osseous extension (arrowhead). **b** Whole body bone scan shows subtle increased activity in the right sacroiliac joint region

reports [40, 41, 53–55]. Most recently, Mujtaba et al. [56] reviewed the literature with regard to imaging features of skeletal metastases from MLS. They suggested that skeletal staging should be considered in MLS, due to the relatively high incidence of bone metastases reported in the literature. However, it should be noted that the rate of metastatic disease at presentation is low, and the relatively high rate of incidental findings on WB-MRI in the young adult population will result in further imaging studies for clarification [57], which contributes to patient anxiety.

Whole-body MRI for distant staging

MLS is unique regarding its unusual pattern of metastatic spread, including extra-pulmonary sites in addition to skeletal deposits. Jagannathan et al. [58] stated that osseous metastases although easily identified by MRI are difficult to diagnose on CT and PET-CT secondary to the lack of significant osseous destruction and prominent myxoid matrix leading to reduced FDG avidity. Therefore, whole-body MRI (WB-MRI) has been investigated for staging of patients with extremity MLS by several authors [50, 59–61]. Stevenson et al. [59] reviewed the efficacy of WB-MRI in 28 patients with MLS treated between 2007 and 2015. All patients had CT studies performed which were compared to 33 WB-MRI studies, and 38 metastases were identified in 7 patients by WB-MRI. Osseous lesions were most common, involving the spine, pelvis (Fig. 6), chest wall, and long bones, followed by soft-tissue and abdominal metastases. Of the 29 bone or soft-tissue metastases that were within the field-of-view on CT, 5 soft-tissue and 0 bone metastases were identified. Metastatic disease was detected in 3 patients purely on WB-MRI which directly influenced management. Based on these findings, they suggested that WB-MRI should be used in two situations: firstly, at diagnosis where ablative treatment such as amputation would be required for cure but the diagnosis of occult metastases would change treatment and secondly at the diagnosis of recurrence to determine if it is a solitary site prior to consideration of metastasectomy. Gorelik et al. [60] undertook a retrospective review of all patients with MLS who underwent WB-MRI for initial staging and routine follow-up between 2006 and 2016. A total of 33 patients with a total of 150 WB-MRI examinations were reviewed. Nine patients (27%) were diagnosed with metastases at a median time of 10 months (range 0–60 months) from diagnosis of the primary tumour. The initial site of metastasis was extra-pulmonary in all cases, with only 2 patients who developed pulmonary metastases diagnosed on chest CT 9 and 29 months after the diagnosis of extra-pulmonary metastases. The first metastasis was diagnosed by WB-MRI in 7 patients (78%), by chest CT in 1 patient, and by abdominal CT in 1 patient. Eight of 9 patients (89%) were asymptomatic at the time of diagnosis of metastases, while in 7 patients (78%), WB-MRI demonstrated metastases included within the field of view of but occult on a contemporaneous CT scan. Gouin et al. [50] undertook a study aimed at describing metastatic patterns on WB-MRI and outcomes in 45 patients with trunk and extremity MLS. Initial WB-MRI was performed within 6 months following the first treatment and then annually. At final follow-up, 10 patients (22.2%) had an extra-pulmonary soft-tissue, or/and bone metastasis is identified at a median time of 22.7 months (range 0–49 months) from diagnosis, of whom 9 were asymptomatic. All patients with metastases had multiple lesions within a year following diagnosis of MLS. Finally, Chien et al. [61] described their experience of 9 patients with MLS diagnosed from 2012 to 2018 who underwent WB-MRI. The focus of their study was to show that STIR sequences alone were adequate for demonstrating metastases (Fig. 13), potentially resulting in significant time-saving. As with other studies, the failure of CT to identify bone metastases was noted.

Therefore, it would appear reasonable from the above data to perform WB-MRI for the initial staging and subsequent surveillance of patients diagnosed with MLS. However, it is questionable whether the identification of asymptomatic metastatic disease will alter management, and it may be a more pragmatic strategy to perform WB-MRI in patients who have been diagnosed with bone metastases to fully stage the skeleton. It is also unclear whether WB-MRI can replace contrast-enhanced CT of the abdomen and pelvis, which could be the subject of further research.

MRI features of post-treatment changes

Both radiotherapy and chemotherapy are used in the management of MLS [62–64]. Radiotherapy is used both pre- and post-operatively for early-stage disease and for palliation of metastatic disease. Chemotherapy is predominantly used for palliation of metastatic disease. MRI has been used to assess response to both treatment modalities.

Pre- and post-operative radiotherapy is commonly used in the management of high-grade STS [65]. Treatment response in terms of changes in tumour volume following pre-operative radiotherapy and percentage tumour necrosis from resection specimens has been described for all sub-types of STS [66, 67], as well as for MLS specifically [17, 19, 68]. Roberge et al. [66] studied 50 patients with a variety of STS who all underwent MRI before and after neo-adjuvant external beam radiotherapy. Tumour volumes were measured on post-contrast T1W sequences while pathological treatment response was measured in terms of percentage of treatment-related necrosis. The latter varied from 0 to 100%, the median being 67.5% for low-grade STS and 50% for high-grade STS. The median decrease in tumour volume was 13.8% for non-myxoid low-grade STS, 82.1% for MLS (Figs. 5,17) and < 1% for high-grade STS. A partial response on MRI (volume

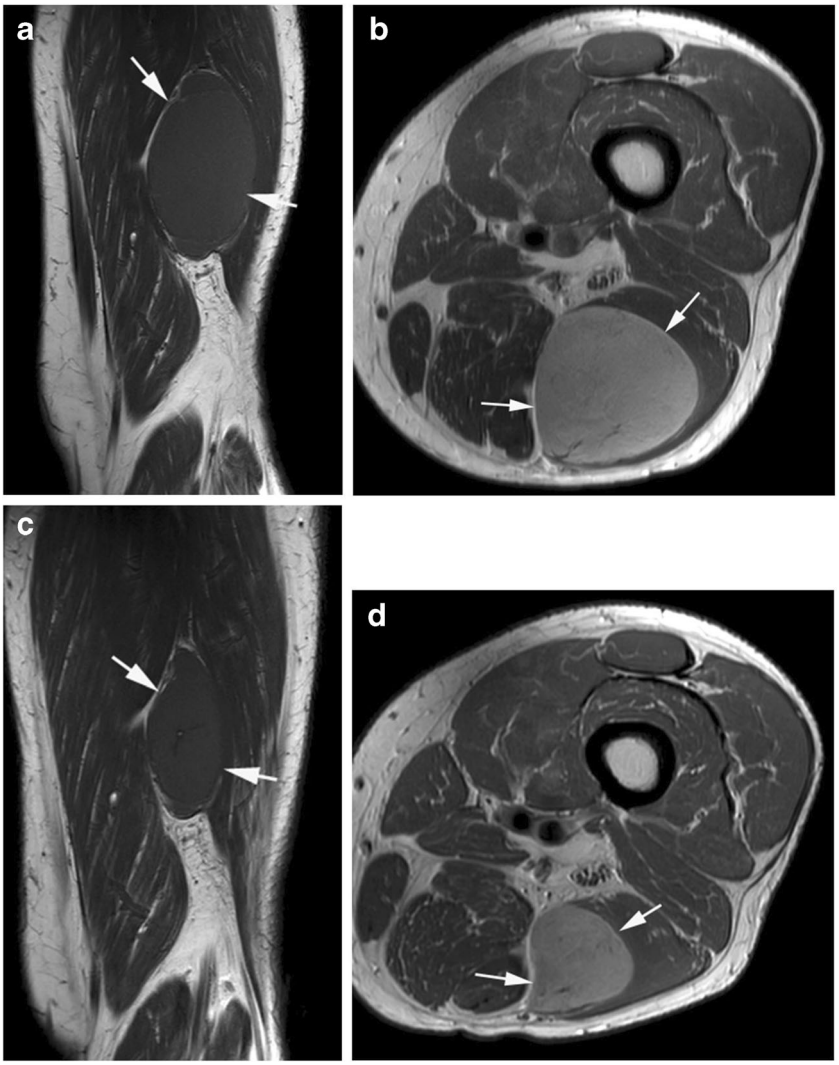

Fig. 17 A 59-year-old male presenting with a mass in the posterior aspect of the left mid-thigh. **a** Coronal T1W TSE and **b** axial PDW FSE MR images show a well-defined, oval mass (arrows) which is slightly hyperintense to muscle on T1W and hyperintense on PDW. **c** Coronal T1W TSE and **d** axial PDW FSE MR images obtained 4 months later after neoadjuvant radiotherapy which resulted in 65% volume reduction of the mass (arrows). Histology confirmed myxoid liposarcoma with no round cell component

reduction ≥50%) was highly predictive of a good pathological response ($p < 0.001$), but patients with no volume reduction or volume increase had wide ranging pathological responses. Le Grange et al. [67] evaluated tumour volume changes after pre-operative radiotherapy for 68 patients with borderline operable STS treated from 2004 to 2011. The median tumour size was 12.5 cm and STS were located in the extremities (87%), trunk (12%), and neck (1%). The commonest histological subtypes were MLS (32%) and myxofibrosarcoma (16%). Post-radiotherapy imaging was available in 55 cases. Tumour volumes reduced in 80% of cases, the median reduction in maximal tumour dimension being 13.6% while the median reduction in tumour volume was 33.3% for all STS subtypes. However, greater reductions were seen for MLS, with median reductions for diameter and volume of 21.4% and − 64.2%, respectively. Adipocytic maturation is seen in MLS following radiotherapy as well as chemotherapy (Fig. 5) [14], and this has been demonstrated on post-radiotherapy MRI using the Dixon technique [69].

Turpin et al. [70] reported the case of a 63-year-old female with a bulky primary MLS and metastatic disease treated with trabectedin as first-line therapy, which resulted in calcification of the primary tumour and the metastases. Crombe et al. [71] described the phenomenon of MRI adipocytic maturation (MAM) following chemotherapy for MLS. Of the 89 patients diagnosed with MLS between 2008 and 2018, 28 were treated with chemotherapy, surgery, and radiotherapy. All patients underwent contrast-enhanced MRI at baseline and follow-up and were compared with 13 patients with either PM-LS or DD-LS who were treated identically. MAM was commoner in MLS ($p = 0.045$), but not specific of any type of chemotherapy ($p = 0.7$). Of the 28 MLS patients, 14 demonstrated MAM, while 8 showed metastatic relapses. MAM was not associated with metastatic relapse-free survival ($p = 0.9$) but correlated strongly with the percentage of histological adipocytic differentiation on resection specimens ($p < 0.001$). They concluded that MAM was a neutral event following chemotherapy, and was not associated with improved metastasis-free survival.

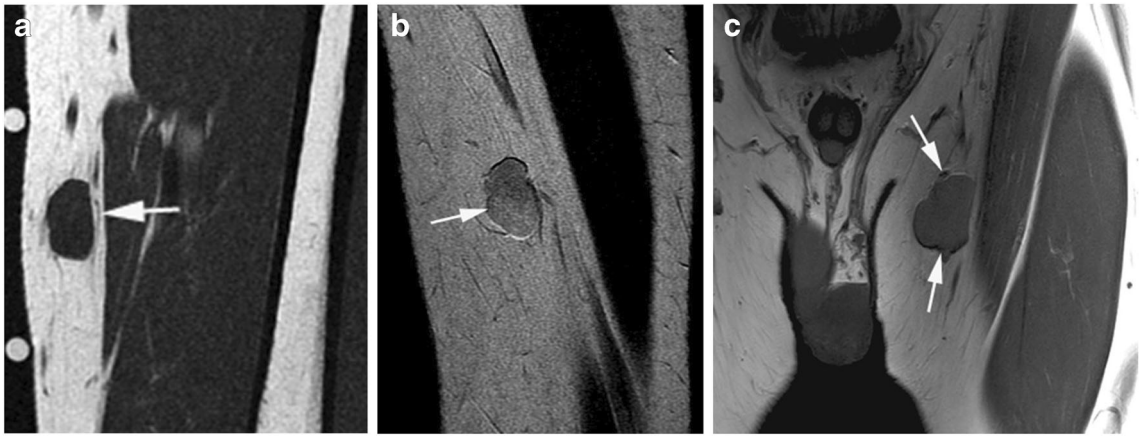

Fig. 18 A 26-year-old male presenting with a small mass in the medial subcutaneous tissues of the left mid-thigh. **a** Coronal T1W TSE and **b** sagittal T2W FSE MR images show a small intermediate SI mass (arrows) in the subcutaneous fat of the medial left thigh with no distinctive features. Histology confirmed myxoid liposarcoma with a round cell component. The patient developed a new mass in the left groin 4 years later. **c** Coronal T1W TSE MR image of the left groin shows an intermediate SI mass (arrows) confirmed to represent recurrent high-grade myxoid liposarcoma

In the situation of incomplete surgical resection following neoadjuvant radiotherapy, re-resection of the surgical bed is usually undertaken at approximately 2 weeks. If further early surgery is not felt to be indicated, then repeat MRI of the surgical site should be undertaken to identify macroscopic residual/recurrent disease and aid surgical re-resection if required. This could be delayed for 3–6 months to allow clearer differentiation of residual/recurrent tumour from post-operative changes, without compromising overall prognosis.

Differential diagnosis of MLS

As previously noted, the detection of a small amount of septal or nodular fatty tissue within a tumour which has a predominantly myxoid matrix allows a prospective MRI diagnosis of MLS in 78–95% of cases [23]. However, the specificity of 'septal fat' for a diagnosis of MLS has not been investigated. A 'cystic' appearing lesion with the absence of any fatty tissue (Fig. 7) or a purely solid appearing tumour (Fig. 18) has a wide differential diagnosis. The differential diagnosis of 'cystic' or 'myxoid' extremity soft tissue masses has been described in several review articles and includes non-neoplastic and benign lesions such as soft tissue ganglia, synovial cysts/bursae, intramuscular myxoma, aggressive angiomyxoma, and benign nerve sheath tumours that have undergone ancient change, as well as sarcomas such as myxofibrosarcoma, low-grade fibromyxoid sarcoma, myxoinflammatory fibroblastic sarcoma, ossifying fibromyxoid tumour, extra-skeletal myxoid chondrosarcoma, and myxoid leiomyosarcoma [72–75]. Harish et al. [76] reviewed 40 consecutive patients with 'cyst-like' appearances on non-contrast MRI who had been referred to a specialist musculoskeletal oncology service, 27 (67.5%) of which were benign. Statistically significant MRI features

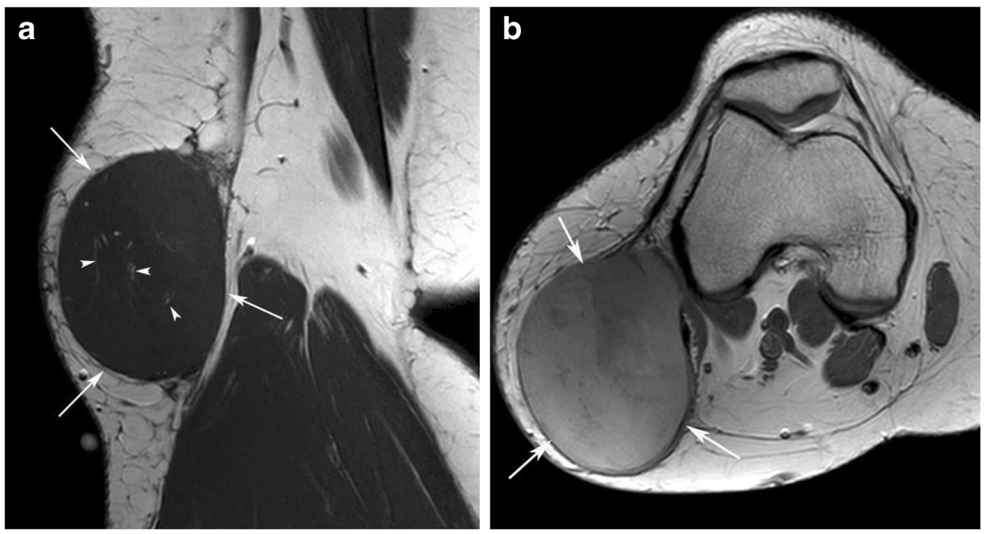

Fig. 19 A 37-year-old female presenting with a large mass in the posterolateral subcutaneous tissues of the left knee. **a** Coronal T1W TSE and **b** axial PDW FSE MR images show a well-defined oval mass (arrows) which contains linear and nodular areas of fat SI (arrowheads-a), based on which an imaging diagnosis of myxoid liposarcoma was suggested. However, resection revealed a monophasic fibrous-type high-grade synovial sarcoma

favouring a diagnosis of malignancy included larger average tumour dimension, larger greatest tumour dimension, and heterogeneity on T1W sequences. The commonest non-malignant diagnoses were myxoma ($n = 16$) and ganglia ($n = 8$), while the 13 STSs included high-grade spindle cell sarcoma ($n = 2$), myxofibrosarcoma ($n = 5$), low-grade fibromyxoid sarcoma ($n = 1$), MLS ($n = 2$), undifferentiated pleomorphic sarcoma ($n = 2$), and myxoid sarcoma unclassified ($n = 1$). Other soft tissue sarcomas that demonstrate linear/septal fat SI on T1W MR images can also mimic MLS (Fig. 19).

Conclusions

This article has reviewed the role of MRI in the initial diagnosis, staging, and subsequent management of MLS. MRI of low-grade MLS commonly demonstrates classical appearances while the presence of a RC component indicating high-grade MLS can also be suggested. WB-MRI is of value for identifying the unusual pattern of predominantly extrapulmonary metastatic disease, particularly bony disease at presentation and follow-up, this being more sensitive for the identification of skeletal metastases compared to radiography, scintigraphy, CT, and FDG-PET.

Declarations

Conflict of interest The authors declare no competing interests.

References

1. Creytens D. What's new in adipocytic neoplasia? Virchows Arch Int J Pathol. 2020 Jan;476(1):29–39.
2. IARC Publications Website - Home [Internet]. [cited 2021 Feb 15]. Available from: https://publications.iarc.fr/588.
3. Kransdorf MJ. Malignant soft-tissue tumors in a large referral population: distribution of diagnoses by age, sex, and location. AJR Am J Roentgenol. 1995 Jan;164(1):129–34.
4. Ye L, Hu C, Wang C, Yu W, Liu F, Chen Z. Nomogram for predicting the overall survival and cancer-specific survival of patients with extremity liposarcoma: a population-based study. BMC Cancer. 2020 Sep 16;20(1):889.
5. Lansu J, Van Houdt WJ, Schaapveld M, Walraven I, Van de Sande MAJ, Ho VKY, et al. Time trends and prognostic factors for overall survival in myxoid liposarcomas: a population-based study. Sarcoma. 2020;2020:2437850.
6. Alaggio R, Coffin CM, Weiss SW, Bridge JA, Issakov J, Oliveira AM, et al. Liposarcomas in young patients: a study of 82 cases occurring in patients younger than 22 years of age. Am J Surg Pathol. 2009 May;33(5):645–58.
7. Abaricia S, Hirbe AC. Diagnosis and treatment of myxoid liposarcomas: histology matters. Curr Treat Options in Oncol. 2018 Oct 25;19(12):64.
8. Abdelfatah E, Guzzetta AA, Nagarajan N, Wolfgang CL, Pawlik TM, Choti MA, et al. Long-term outcomes in treatment of retroperitoneal sarcomas: a 15 year single-institution evaluation of prognostic features. J Surg Oncol. 2016 Jul;114(1):56–64.
9. Song T, Shen J, Liang BL, Mai WW, Li Y, Guo HC. Retroperitoneal liposarcoma: MR characteristics and pathological correlative analysis. Abdom Imaging. 2007 Oct;32(5):668–74.
10. de Vreeze RSA, de Jong D, Tielen IHG, Ruijter HJ, Nederlof PM, Haas RL, et al. Primary retroperitoneal myxoid/round cell liposarcoma is a nonexisting disease: an immunohistochemical and molecular biological analysis. Mod Pathol Off J U S Can Acad Pathol Inc. 2009 Feb;22(2):223–31.
11. Weingertner N, Neuville A, Chibon F, Ray-Coquard I, Marcellin L, Ghnassia J-P. Myxoid liposarcoma with heterologous components: dedifferentiation or metaplasia? A FISH-documented and CGH-documented case report. Appl Immunohistochem Mol Morphol AIMM. 2015 Mar;23(3):230–5.
12. Ioannou MG, Kouvaras E, Papamichali R, Karachalios T, Koukoulis G. Myxoid liposarcoma with cartilaginous differentiation: a case study with fish analysis and review of the literature. Pathol Res Pract. 2013 Oct;209(10):666–9.
13. Enzinger and Weiss's Soft Tissue Tumors - 7th Edition [Internet]. [cited 2021 Feb 15]. Available from: https://www.elsevier.com/books/enzinger-and-weisss-soft-tissue-tumors/goldblum/978-0-323-61096-4
14. Moreau L-C, Turcotte R, Ferguson P, Wunder J, Clarkson P, Masri B, et al. Myxoid\round cell liposarcoma (MRCLS) revisited: an analysis of 418 primarily managed cases. Ann Surg Oncol. 2012 Apr;19(4):1081–8.
15. Hoffman A, Ghadimi MPH, Demicco EG, Creighton CJ, Torres K, Colombo C, et al. Localized and metastatic myxoid/round cell liposarcoma: clinical and molecular observations. Cancer. 2013 May 15;119(10):1868–77.
16. Narendra S, Valente A, Tull J, Zhang S. DDIT3 gene break-apart as a molecular marker for diagnosis of myxoid liposarcoma–assay validation and clinical experience. Diagn Mol Pathol Am J Surg Pathol Part B. 2011 Dec;20(4):218–24.
17. Salduz A, Alpan B, Valiyev N, Özmen E, İribaş A, Ağaoğlu F, et al. Neoadjuvant radiotherapy for myxoid liposarcomas: oncologic outcomes and histopathologic correlations. Acta Orthop Traumatol Turc. 2017 Oct;51(5):355–61.
18. Koseła-Paterczyk H, Spałek M, Borkowska A, Teterycz P, Wągrodzki M, Szumera-Ciećkiewicz A, et al. Hypofractionated radiotherapy in locally advanced myxoid liposarcomas of extremities or trunk wall: results of a single-arm prospective clinical trial. J Clin Med [Internet]. 2020 Aug 1 [cited 2021 Feb 15];9(8). Available from: https://www.ncbi.nlm.nih.gov/pmc/articles/PMC7464815/
19. Lansu J, Bovee JVMG, Braam P, van Boven H, Flucke U, Bonenkamp JJ, et al. Dose reduction of preoperative radiotherapy in myxoid liposarcoma a nonrandomized controlled trial. JAMA Oncol. 2021;7(1):1–8.
20. Barile A, Zugaro L, Catalucci A, Caulo M, Di Cesare E, Splendiani A, et al. Soft tissue liposarcoma: histological subtypes, MRI and CT findings. Radiol Med (Torino). 2002;104(3):140–9.
21. El Ouni F, Jemni H, Trabelsi A, Ben Maitig M, Arifa N, Ben Rhouma K, et al. Liposarcoma of the extremities: MR imaging features and their correlation with pathologic data. Orthop Traumatol Surg Res OTSR. 2010;96(8):876–83.
22. Wortman JR, Tirumani SH, Jagannathan JP, Tirumani H, Shinagare AB, Hornick JL, et al. Primary extremity liposarcoma: MRI features, histopathology, and clinical outcomes. J Comput Assist Tomogr. 2016;40(5):791–8.
23. Murphey MD, Arcara LK, Fanburg-Smith J. From the archives of the AFIP: imaging of musculoskeletal liposarcoma with radiologic-pathologic correlation. Radiogr Rev Publ Radiol Soc N Am Inc. 2005;25(5):1371–95.

24. Saifuddin A, Siddiqui S, Pressney I, Khoo M. The incidence and diagnostic relevance of chemical shift artefact in the magnetic resonance imaging characterisation of superficial soft tissue masses. Br J Radiol. 2020;93(1108):20190828.
25. Sundaram M, Baran G, Merenda G, McDonald DJ. Myxoid liposarcoma: magnetic resonance imaging appearances with clinical and histological correlation. Skelet Radiol. 1990;19(5):359–62.
26. Sung MS, Kang HS, Suh JS, Lee JH, Park JM, Kim JY, et al. Myxoid liposarcoma: appearance at MR imaging with histologic correlation. Radiogr Rev Publ Radiol Soc N Am Inc. 2000;20(4):1007–19.
27. Lunn BW, Littrell LA, Wenger DE, Broski SM. 18F-FDG PET/CT and MRI features of myxoid liposarcomas and intramuscular myxomas. Skelet Radiol. 2018;47(12):1641–50.
28. Tateishi U, Hasegawa T, Beppu Y, Kawai A, Satake M, Moriyama N. Prognostic significance of MRI findings in patients with myxoid-round cell liposarcoma. AJR Am J Roentgenol. 2004;182(3):725–31.
29. Kuyumcu G, Rubin BP, Bullen J, Ilaslan H. Quantification of fat content in lipid-rich myxoid liposarcomas with MRI: a single-center experience with survival analysis. Skelet Radiol. 2018;47(10):1411–7.
30. Crombé A, Le Loarer F, Sitbon M, Italiano A, Stoeckle E, Buy X, et al. Can radiomics improve the prediction of metastatic relapse of myxoid/round cell liposarcomas? Eur Radiol. 2020;30(5):2413–24.
31. Löwenthal D, Zeile M, Niederhagen M, Fehlberg S, Schnapauff D, Pink D, et al. Differentiation of myxoid liposarcoma by magnetic resonance imaging: a histopathologic correlation. Acta Radiol Stockh Swed 1987. 2014;55(8):952–60.
32. Gimber LH, Montgomery EA, Morris CD, Krupinski EA, Fayad LM. MRI characteristics associated with high-grade myxoid liposarcoma. Clin Radiol. 2017;72(7):613.e1–6.
33. Levy AD, Manning MA, Al-Refaie WB, Miettinen MM. Soft-tissue sarcomas of the abdomen and pelvis: radiologic-pathologic features, part 1-common sarcomas: from the radiologic pathology archives. Radiogr Rev Publ Radiol Soc N Am Inc. 2017 Apr;37(2):462–83.
34. Pearlstone DB, Pisters PW, Bold RJ, Feig BW, Hunt KK, Yasko AW, et al. Patterns of recurrence in extremity liposarcoma: implications for staging and follow-up. Cancer. 1999;85(1):85–92.
35. Estourgie SH, Nielsen GP, Ott MJ. Metastatic patterns of extremity myxoid liposarcoma and their outcome. J Surg Oncol. 2002;80(2):89–93.
36. Schwab JH, Boland P, Guo T, Brennan MF, Singer S, Healey JH, et al. Skeletal metastases in myxoid liposarcoma: an unusual pattern of distant spread. Ann Surg Oncol. 2007;14(4):1507–14.
37. Asano N, Susa M, Hosaka S, Nakayama R, Kobayashi E, Takeuchi K, et al. Metastatic patterns of myxoid/round cell liposarcoma: a review of a 25-year experience. Sarcoma. 2012;2012:345161.
38. Dürr HR, Rauh J, Baur-Melnyk A, Knösel T, Lindner L, Roeder F, et al. Myxoid liposarcoma: local relapse and metastatic pattern in 43 patients. BMC Cancer. 2018;18(1):304.
39. Smolle MA, Leithner A, Bernhardt GA. Abdominal metastases of primary extremity soft tissue sarcoma: a systematic review. World J Clin Oncol. 2020;11(2):74–82.
40. Ishii T, Ueda T, Myoui A, Tamai N, Hosono N, Yoshikawa H. Unusual skeletal metastases from myxoid liposarcoma only detectable by MR imaging. Eur Radiol. 2003;13(Suppl 4):L185–91.
41. Hanna SA, Qureshi YA, Bayliss L, David LA, O'Donnell P, Judson IR, et al. Late widespread skeletal metastases from myxoid liposarcoma detected by MRI only. World J Surg Oncol. 2008;6:62.
42. Zagzoog N, Ra G, Koziarz A, Provias J, Sommer D, Almenawer SA, et al. Metastatic liposarcoma of the skull base: a case report and review of literature. Neurosurgery. 2017;80(4):219–23.
43. Ng C, Stebbing J, Judson I. Cardiac metastasis from a myxoid liposarcoma. Clin Oncol R Coll Radiol G B. 2001;13(5):384–5.
44. Aoyama A, Isowa N, Chihara K, Ito T. Pericardial metastasis of myxoid liposarcoma causing cardiac tamponade. Jpn J Thorac Cardiovasc Surg Off Publ Jpn Assoc Thorac Surg Nihon Kyobu Geka Gakkai Zasshi. 2005 Apr;53(4):193–5.
45. Motevalli D, Tavangar SM. Extensive left ventricular, pulmonary artery, and pericardial metastasis from myxoid liposarcoma 16 years after the initial detection of the primary tumour: a case report and review of the literature. Malays J Pathol. 2017;39(2):201–5.
46. Yokouchi M, Nagano S, Kijima Y, Yoshioka T, Tanimoto A, Natsugoe S, et al. Solitary breast metastasis from myxoid liposarcoma. BMC Cancer. 2014;14:482.
47. Wang D, Wu J, Yu J, Zhang H, Liu H. Solitary pancreatic metastasis of extremity myxoid liposarcoma: a case report and literature review. BMC Cancer. 2018;18(1):1121.
48. Urakawa H, Nakanishi K, Arai E, Ikuta K, Hamada S, Ota T, et al. Single metastasis of myxoid liposarcoma from the thigh to thyroid gland: a case report. World J Surg Oncol. 2018 Mar 27;16(1):71.
49. Kim D-W, Jee YS. Solitary metastasis of myxoid liposarcoma from the thigh to intraperitoneum: a case report. World J Surg Oncol. 2019;17(1):172.
50. Gouin F, Renault A, Bertrand-Vasseur A, Bouilleau L, Crenn V, Rosset P, et al. Early detection of multiple bone and extra-skeletal metastases by body magnetic resonance imaging (BMRI) after treatment of myxoid/round-cell liposarcoma (MRCLS). Eur J Surg Oncol J Eur Soc Surg Oncol Br Assoc Surg Oncol. 2019;45(12):2431–6.
51. Sheah K, Ouellette HA, Torriani M, Nielsen GP, Kattapuram S, Bredella MA. Metastatic myxoid liposarcomas: imaging and histopathologic findings. Skelet Radiol. 2008;37(3):251–8.
52. Noble JL, Moskovic E, Fisher C, Judson I. Imaging of skeletal metastases in myxoid liposarcoma. Sarcoma. 2010;2010:262361.
53. Schwab JH, Boland PJ, Antonescu C, Bilsky MH, Healey JH. Spinal metastases from myxoid liposarcoma warrant screening with magnetic resonance imaging. Cancer. 2007;110(8):1815–22.
54. Conill C, Setoain X, Colomo L, Palacín A, Combalia-Aleu A, Pomés J, et al. Diagnostic efficacy of bone scintigraphy, magnetic resonance imaging, and positron emission tomography in bone metastases of myxoid liposarcoma. J Magn Reson Imaging JMRI. 2008;27(3):625–8.
55. Sakamoto A, Fukutoku Y, Matsumoto Y, Harimaya K, Oda Y, Iwamoto Y. Myxoid liposarcoma with negative features on bone scan and [18F]-2-fluoro-2-deoxy-D-glucose-positron emission tomography. World J Surg Oncol. 2012;10:214.
56. Mujtaba B, Wang F, Taher A, Aslam R, Madewell JE, Nassar S. Myxoid Liposarcoma with skeletal metastases: pathophysiology and imaging characteristics. Curr Probl Diagn Radiol. 2021;50(1):66–73.
57. du Preez H, Lasker I, Rajakulasingam R, Saifuddin A. Whole-body magnetic resonance imaging: incidental findings in paediatric and adult populations. Eur J Radiol. 2020;130:109156.
58. Jagannathan JP, Tirumani SH, Ramaiya NH. Imaging in soft tissue sarcomas: current updates. Surg Oncol Clin N Am. 2016;25(4):645–75.
59. Stevenson JD, Watson JJ, Cool P, Cribb GL, Jenkins JPR, Leahy M, et al. Whole-body magnetic resonance imaging in myxoid liposarcoma: a useful adjunct for the detection of extra-pulmonary metastatic disease. Eur J Surg Oncol J Eur Soc Surg Oncol Br Assoc Surg Oncol. 2016;42(4):574–80.
60. Gorelik N, Reddy SMV, Turcotte RE, Goulding K, Jung S, Alcindor T, et al. Early detection of metastases using whole-body MRI for initial staging and routine follow-up of myxoid liposarcoma. Skelet Radiol. 2018;47(3):369–79.
61. Chien A, Zuppan CW, Lei L, Williams NL, Shields TG, Elsissy JG, et al. Short tau inversion recovery magnetic resonance imaging for staging and screening in myxoid liposarcoma. J Orthop. 2019;16(3):206–10.

62. Ratan R, Patel SR. Trabectedin and eribulin: where do they fit in the management of soft tissue sarcoma? Curr Treat Options in Oncol. 2017;18(6):34.
63. Chowdhry V, Goldberg S, DeLaney TF, Cote GM, Chebib I, Kim J, et al. Myxoid liposarcoma: treatment outcomes from chemotherapy and radiation therapy. Sarcoma. 2018;2018:8029157.
64. Crago AM, Dickson MA. Liposarcoma: multimodality management and future targeted therapies. Surg Oncol Clin N Am. 2016;25(4):761–73.
65. Yang X, Zhang L, Yang X, Yu W, Fu J. Oncologic outcomes of pre- versus post-operative radiation in resectable soft tissue sarcoma: a systematic review and meta-analysis. Radiat Oncol Lond Engl. 2020;15(1):158.
66. Roberge D, Skamene T, Nahal A, Turcotte RE, Powell T, Freeman C. Radiological and pathological response following pre-operative radiotherapy for soft-tissue sarcoma. Radiother Oncol J Eur Soc Ther Radiol Oncol. 2010;97(3):404–7.
67. le Grange F, Cassoni AM, Seddon BM. Tumour volume changes following pre-operative radiotherapy in borderline resectable limb and trunk soft tissue sarcoma. Eur J Surg Oncol J Eur Soc Surg Oncol Br Assoc Surg Oncol. 2014;40(4):394–401.
68. Koseła-Paterczyk H, Szumera-Ciećkiewicz A, Szacht M, Haas R, Morysiński T, Dziewirski W, et al. Efficacy of neoadjuvant hypofractionated radiotherapy in patients with locally advanced myxoid liposarcoma. Eur J Surg Oncol J Eur Soc Surg Oncol Br Assoc Surg Oncol. 2016;42(6):891–8.
69. Skorpil M, Rydén H, Wejde J, Lidbrink E, Brosjö O, Berglund J. The effect of radiotherapy on fat content and fatty acids in myxoid liposarcomas quantified by MRI. Magn Reson Imaging. 2017;43:37–41.
70. Turpin A, Taieb S, Penel N. Tumor calcification: a new response pattern of myxoid liposarcoma to trabectedin. Case Rep Oncol. 2014;7(1):204–9.
71. Crombe A, Sitbon M, Stoeckle E, Italiano A, Buy X, Le Loarer F, et al. Magnetic resonance imaging assessment of chemotherapy-related adipocytic maturation in myxoid/round cell liposarcomas: specificity and prognostic value. Br J Radiol. 2020;93(1110):20190794.
72. Bermejo A, De Bustamante TD, Martinez A, Carrera R, Zabía E, Manjón P. MR imaging in the evaluation of cystic-appearing soft-tissue masses of the extremities. Radiogr Rev Publ Radiol Soc N Am Inc. 2013;33(3):833–55.
73. Thawait GK, Subhawong TK, Tatizawa Shiga NY, Fayad LM. 'Cystic'-appearing soft tissue masses: what is the role of anatomic, functional, and metabolic MR imaging techniques in their characterization? J Magn Reson Imaging JMRI. 2014;39(3):504–11.
74. Petscavage-Thomas JM, Walker EA, Logie CI, Clarke LE, Duryea DM, Murphey MD. Soft-tissue myxomatous lesions: review of salient imaging features with pathologic comparison. Radiogr Rev Publ Radiol Soc N Am Inc. 2014;34(4):964–80.
75. Baheti AD, Tirumani SH, Rosenthal MH, Howard SA, Shinagare AB, Ramaiya NH, et al. Myxoid soft-tissue neoplasms: comprehensive update of the taxonomy and MRI features. AJR Am J Roentgenol. 2015;204(2):374–85.
76. Harish S, Lee JC, Ahmad M, Saifuddin A. Soft tissue masses with 'cyst-like' appearance on MR imaging: distinction of benign and malignant lesions. Eur Radiol. 2006;16(12):2652–60.